Preparation and activity evaluation of p–n junction photocatalyst NiO/TiO$_2$

Chen Shifu [*], Zhang Sujuan, Liu Wei, Zhao Wei

Department of Chemistry, Huaibei Coal Normal College, Anhui, Huaibei 235000, People's Republic of China

Abstract

p–n Junction photocatalyst NiO/TiO$_2$ was prepared by sol–gel method using Ni(NO$_3$)$_2$·6H$_2$O and tetrabutyl titanate [Ti(OC$_4$H$_9$)$_4$] as the raw materials. The p–n junction photocatalyst NiO/TiO$_2$ was characterized by UV–vis diffuse reflection spectrum, X-ray powder diffraction (XRD) and X-ray photoelectron spectroscopy (XPS). The photocatalytic activity of the photocatalyst was evaluated by photocatalytic reduction of Cr$_2$O$_7^{2-}$ and photocatalytic oxidation of rhodamine B. The results show that, for photocatalytic reduction of Cr$_2$O$_7^{2-}$, the optimum percentage of doped-NiO is 0.5% (mole ratio of Ni/Ti). The photocatalytic activity of the p–n junction NiO/TiO$_2$ is much higher than that of TiO$_2$ on the photocatalytic reduction of Cr$_2$O$_7^{2-}$. However, the photocatalytic activity of the p–n junction photocatalyst NiO/TiO$_2$ is much lower than that of TiO$_2$ on the photocatalytic oxidation of rhodamine B. Namely, the p–n junction photocatalyst NiO/TiO$_2$ has higher photocatalytic reduction activity, but lower photocatalytic oxidation activity. Effects of heat treatment on the photocatalytic activity of p–n junction photocatalyst NiO/TiO$_2$ were investigated. The mechanisms of influence on the photocatalytic activity were also discussed by the p–n junction principle.
© 2007 Elsevier B.V. All rights reserved.

Keywords: NiO/TiO$_2$; p–n Junction; Photocatalyst; Activity; Characterization

1. Introduction

In recent years, the photocatalytic degradation of various kinds of organic and inorganic pollutants using semiconductor powders as photocatalysts has been extensively studied [1–4]. Owing to its relatively high photocatalytic activity, biological and chemical stability, low cost, non-toxic nature and long-term stability, TiO$_2$ has been widely used as a photocatalyst [5,6]. However, the photocatalytic activity of TiO$_2$ (the band gap of anatase TiO$_2$ is 3.2 eV and it can be excited by photons with wavelengths below 387 nm) is limited to irradiation wavelengths in the UV region, thereby the effective utilization of solar energy is limited to about 3–5% of the total solar spectrum. Some problems still remain to be solved in its application, such as the fast recombination of photogenerated electron–hole pairs. Therefore, improving photocatalytic activity by modification has become a hot topic among researchers in recent years [7,8]. One approach is to dope transition metals into TiO$_2$, and the other is to form coupled photocatalysts [9,10]. Recently, it was found that substitution of a non-metallic element such as nitrogen, fluorine, sulfur, carbon, etc., for oxygen in the TiO$_2$ lattice is more efficient in improving its photocatalytic activity in the visible region [6,11–14]. Doping of metal ions, such as Ag$^+$, Cu^{2+}, Fe^{3+}, etc., has been widely employed to enhance the photocatalytic activity of TiO$_2$ [15–18]. Doped-NiO into semiconductors, such as TiO$_2$, InVO$_4$, NaTaO$_3$, etc., has been reported in a few literatures [19,20]. But the photocatalysts were usually applied to produce hydrogen and oxygen from water. The results show that the efficiency of photocatalytic splitting of water for the doped-NiO photocatalyst was higher than that of pure semiconductor photocatalysts. It was proposed that oxide nickel facilitate the photoexcited electrons transfer and hence suppress recombination of photogenerated electron and hole.

It is known that NiO is p-type semiconductor [21,22], and TiO$_2$ is n-type semiconductor. When p-type NiO and n-type TiO$_2$ integrates, a p–n junction will be formed between p-NiO and n-TiO$_2$. Theoretically, when p-type semiconductor NiO and n-type semiconductor TiO$_2$ form p–n junctions, the inner electric field will be formed in the interface. At the equilibrium, the inner electric field makes p-type semiconductor NiO region have

---

[*] Corresponding author. Tel.: +86 561 3803279; fax: +86 561 3803141.
E-mail address: chshifu@hbcnc.edu.cn (C. Shifu).

the negative charge, while TiO_2 region have the positive charge. Under near UV illumination, electron–hole pairs may be created on the n-type semiconductor TiO_2 surface, and the photogenerated electron–hole pairs are separated by the inner electric field. The holes flow into the negative field and the electrons move to the positive field. As a result, the photogenerated electrons and holes are separated efficiently, and the photocatalytic activity is enhanced.

In this study, the p–n junction photocatalyst NiO/TiO_2 was prepared by the sol–gel method using $Ni(NO_3)_2 \cdot 6H_2O$ and tetrabutyl titanate $[Ti(OC_4H_9)_4]$ as the raw materials. The p–n junction photocatalyst NiO/TiO_2 was characterized by UV–vis diffuse reflection spectrum, X-ray powder diffraction (XRD) and X-ray photoelectron spectroscopy (XPS). The photocatalytic activity of the photocatalysts was evaluated by photocatalytic reduction of $Cr_2O_7{}^{2-}$ and photocatalytic oxidation of rhodamine B. Effect of heat treatment on the photocatalytic activity of p–n junction photocatalyst NiO/TiO_2 was discussed. The possible mechanisms of p–n junction formation and separation of photoexcited electron and hole were also investigated.

2. Experimental

2.1. Materials

Tetrabutyl titanate $[Ti (OC_4H_9)_4]$ was prepared in our laboratory. *N*-butyl alcohol, ethyl alcohol, potassium dichromate $(K_2Cr_2O_7)$, $Ni(NO_3)_2 \cdot 6H_2O$, rhodamine B and other chemicals used in the experiments were of analytically pure grade. They were purchased from Shanghai and other China Chemical Reagent Ltd. without further purification. Deionized water was used throughout this study.

2.2. Preparation of p–n junction photocatalyst NiO/TiO_2

Precursor solutions for TiO_2 powder were prepared at the room temperature by the sol–gel method described in Refs. [23,24]. A 50 ml tetrabutyl titanate was dissolved in 100 ml n-butanol, and stirred vigorously for 1 h, assigned as solution A. Quantitative $Ni(NO_3)_2 \cdot 6H_2O$ solution was mixed with 200 ml ethyl alcohol and dilute nitric acid (HNO_3), assigned as solution B. Then, the mixture B was added dropwise into solution A. The above solutions that meet the previously designed mole ratio of Ni/Ti with 0.0, 0.05, 0.1, 0.5, 1.0, 2.0, 10.0 and 20.0% were prepared, respectively. The colloidal solutions formed were dried at room temperature for 24 h in a dust-free environment before heat treatment. Finally, the colloidal powders were heated in air at 400, 500, 550, 600 and 700 °C for 2, 3, 4 and 6 h, respectively. In this way, different kinds of p–n junction photocatalyst NiO/TiO_2 powder samples were prepared.

2.3. Photoreaction apparatus and procedure

Experiments were carried out in a photoreaction apparatus. The schematic diagram is shown in Fig. 1. The photoreaction apparatus consists of two parts. The first part is an annular quartz tube. A 375 W medium pressure mercury lamp (Institute
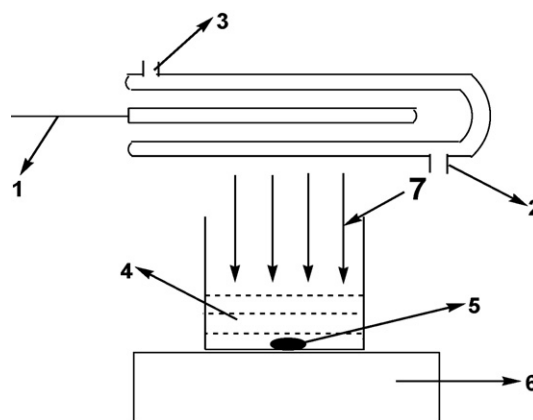

Fig. 1. Schematic diagram of photoreaction apparatus. (1) lamp; (2) water-cooling inlet; (3) water-cooling outlet; (4) reaction solution; (5) stirring rod; (6) magnetic agitator; and (7) light.

of Electric Light Source, Beijing) with a maximum emission at about 365 nm is hung in the empty chamber of the annular tube, and running water passing through an inner thimble of the annular tube. Owing to continuous cooling, the temperature of the reaction solution is maintained at approximately 30 °C. The second part is an unsealed beaker of a diameter 12 cm. At the start of the experiment, the reaction solution (volume, 300 cm^3) containing reactants and photocatalyst was put in the unsealed beakers, and using a magneton to stir the reaction solution. The distance between the light source and the surface of the reaction solution is 11 cm. The UV irradiation intensity (the wavelengths below 400 nm) of the reaction solution surface is about 18,300 $\mu W\, cm^{-2}$. In the experiments, the initial pH of the reaction solution was 5.0. The amount of photocatalyst used was 2.0 $g\, L^{-1}$, the initial concentrations of $Cr_2O_7{}^{2-}$ and rhodamine B are 3.8×10^{-4} and $1.0 \times 10^{-4}\, mol\, L^{-1}$, respectively. The illumination time of each experiment was 20 min. In order to disperse the photocatalyst powder, the suspensions were ultrasonically vibrated for 20 min prior to irradiation. After illumination, the samples (volume of each is 5 cm^3) were taken from the reaction suspension, centrifuged at 7000 rpm for 10 min and filtered through a 0.2-μm Millipore filter to remove the particles. The filtrate was then analyzed. In order to determine the reproducibility of the results, at least duplicated runs were carried out for each condition for averaging the results, and the experimental error was found to be within ±4%.

2.4. Characterization

UV–vis diffuse reflectance spectroscopy measurements were carried out using a Hitachi UV-365 spectrophotometer equipped with an integrating sphere attachment. The analysis range was from 300 to 700 nm, and $BaSO_4$ was used as a reflectance standard.

In order to determine the crystal phase composition and the crystallite size of the photocatalysts, X-ray diffraction measurement was carried out at room temperature using a Philips MPD 18801 X-ray powder diffractometer with Cu Kα radiation and a scanning speed of 3°/min. The accelerating voltage and emis-

sion current were 35 kV and 20 mA, respectively. The crystallite size was calculated by X-ray line broadening analysis using the Scherrer equation.

X-ray photoelectron spectroscopic (XPS) examination was carried out on a Thermo ESCALAB 250 multifunctional spectrometer (VG Scientific UK) using Al Kα radiation. All XPS spectra were referenced to the C1s peak at 284.8 eV from the adventitious hydrocarbon contamination.

UV irradiation intensity of the medium pressure mercury lamp was measured by a UV radiometer (UV-A type UV radiometer China).

2.5. Analysis

The concentration of $Cr_2O_7^{2-}$ in solution is determined spectrophotometrically using diphenylcarbazide reagent as a developer. The concentration of rhodamine B in solution is determined spectrophotometrically. 721-type spectrophotometer was used throughout this study.

The photoreduction efficiency of $Cr_2O_7^{2-}$ and the photooxidation efficiency of rhodamine B were calculated from the following expression:

$$\eta = \frac{(C_0 - C_t)}{C_0} \times 100\%,$$

were η is the photocatalytic efficiency; C_0 is the initial concentration of reactant; C_t is the concentration of reactant after illumination time t.

3. Results and discussion

3.1. Effect of amount of doped-NiO on the photocatalytic activity

Fig. 2 shows the effects of amounts of doped-NiO on the photocatalytic reduction of $Cr_2O_7^{2-}$ and photocatalytic oxidation of rhodamine B. The photocatalysts were heated at temperature 550 °C for 2 h, and fixed illumination time for each experiment
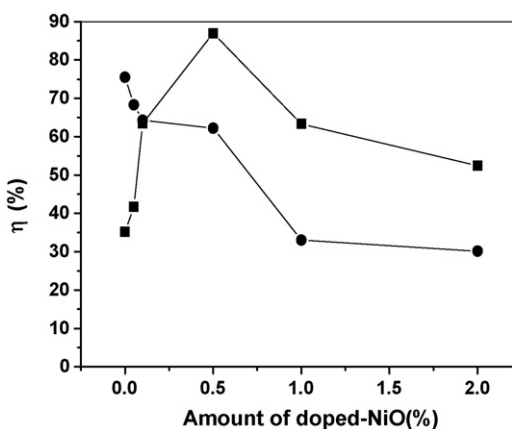

Fig. 2. Effects of amounts of doped-NiO on the photocatalytic reduction of $Cr_2O_7^{2-}$ and photocatalytic oxidation of rhodamine B. (■) $Cr_2O_7^{2-}$; and (●) rhodamine B.

was 20 min. From Fig. 2, it can be seen that, for the photocatalytic reduction of $Cr_2O_7^{2-}$, the photoreduction activity of NiO/TiO$_2$ increases remarkably with the increase in the amounts of doped-NiO up to 0.5% (mole ratio of Ni/Ti). The optimum amount of doped-NiO is 0.5% (mole ratio of Ni/Ti). When the amount of doped is higher than optimal amount, the photoreduction activity of the NiO/TiO$_2$ photocatalyst decreases gradually as the amounts of doped-NiO increases. The results also show that without NiO present, namely, the pure TiO$_2$ powder photocatalyst, its photoreduction activity is the lowest, and the photoreduction efficiency is 35.2%. When the amount of doped-NiO is 0.5% (mole ratio of Ni/Ti), the photoreduction activity of NiO/TiO$_2$ is at its peak, and the photoreduction efficiency is 87.0%. It is clear that the photoreduction activity of doped-NiO (when the mole ratio of Ni/Ti is 0.5%) is two times than that of pure TiO$_2$. However, under the same condition, for the photocatalytic oxidation of rhodamine B, the photooxidation activity of NiO/TiO$_2$ decreases rapidly with the increase in the amounts of doped-NiO up to 0.1%. But when the amount of doped-NiO is from 0.1 to 0.5%, the photooxidation activity of NiO/TiO$_2$ varies slowly. For the pure TiO$_2$ powder photocatalyst, its photooxidation activity is at its peak, the photooxidation efficiency of TiO$_2$ is 75.5%. When the amounts of doped-NiO are 0.5 and 2.0%, the photooxidation efficiencies are 62.2 and 30.1%, respectively.

The possible reasons are as follows. First, an addition of small amount of NiO can prevent the growth of the TiO$_2$ granule, and this made specific surface area of the photocatalyst increases, so the photocatalytic activity increases. For example, when the photocatalysts were heated at temperature 500 °C for 2 h, the specific surface areas of pure TiO$_2$ and NiO (0.5%)/TiO$_2$ are 80.8 and 115.6 m^2/g, respectively. Second, when doping NiO into TiO$_2$ granule, the crystal phase transformation of TiO$_2$ from anatase to rutile is inhibited. It was reported that anatase has a higher photocatalytic oxidation and reduction activity than that of rutile [25,26]. The above results are verified by XRD. Third, it is a great important reason, it is known that NiO is p-type semiconductor and TiO$_2$ is n-type semiconductor. When doping NiO into TiO$_2$ granule, a number of micro p–n junctions NiO/TiO$_2$ photocatalysts will be formed. At the equilibrium, the inner electric field formed which made p-type semiconductor NiO region have the negative charge while TiO$_2$ region have the positive charge. Under near UV illumination, electron–hole pairs may be created on the n-type semiconductor TiO$_2$ surface. With the effect of the inner electric field, the holes flow into the negative field and the electrons move to the positive field. Thus, the photogenerated electron–hole pairs will be separated effectively by the p–n junction formed in the NiO/TiO$_2$. At the same time, it has been reported that p-type NiO species acts as hole traps and collector [27]. Therefore, there were enrichment electrons in the interface to react with $Cr_2O_7^{2-}$ adsorbed on the photocatalyst surface, so the p–n junction photocatalyst NiO/TiO$_2$ has higher photocatalytic reduction activity than that of TiO$_2$, but lower photocatalytic oxidation activity. According to the above observations, the p–n junction formation model and the schematic diagram of electron–hole separation process on the surface of TiO$_2$ are illustrated in Fig. 3.
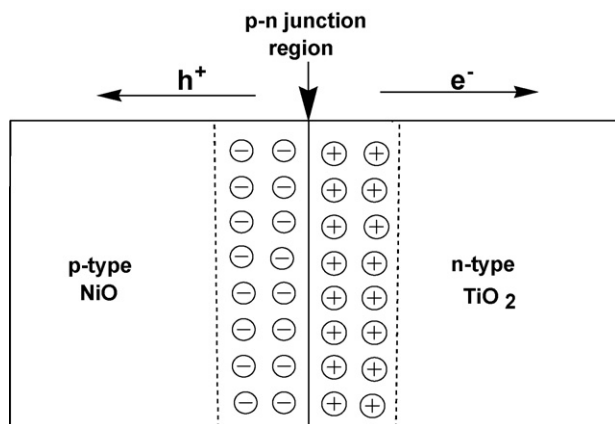
Fig. 3. p–n Junction formation model and the schematic diagram of electron–hole separation process.

Fig. 5. Effect of heat treatment on the photocatalytic oxidation of rhodamin B. (■) p-NiO/n-TiO$_2$; and (●) n-TiO$_2$.

In order to further verify the photocatalytic oxidation activity of the p–n junction photocatalyst NiO/TiO$_2$, the photocatalytic oxidation of methyl orange (MO) and NO$_2^-$ were also studied. The results show that when the amounts of doped-NiO are 0.0, 0.5 and 2.0%, illumination for 20 min, for 1.0×10^{-4} mol L^{-1} of methyl orange (MO), the photooxidation efficiencies are 68.3, 45.8 and 36.6%, respectively; and for 1.0×10^{-4} mol L^{-1} of NO$_2^-$, the photooxidation efficiencies are 33.0, 20.4 and 11.2%, respectively. The conclusion is the same as above. Namely, the photooxidation activity of NiO/TiO$_2$ decreases gradually with the increase in the amounts of doped-NiO.

3.2. Effect of heat treatment on the photocatalytic activity

The fixed amount of doped-NiO in the sample is 0.5% (mole ratio of Ni/Ti). Effects of heat treatment on the photocatalytic reduction of Cr$_2$O$_7^{2-}$ and the photocatalytic oxidation of rhodamine B are shown in Figs. 4 and 5, respectively. It can be seen that the photocatalytic activity of NiO/TiO$_2$ varies with different heat treatment temperatures and time. From Fig. 4, it is clear that, under the experimental condition, the photocatalytic reduction activity of NiO/TiO$_2$ is greater than that of pure TiO$_2$. However, from Fig. 5, it is clear that the photocatalytic oxidation activity of NiO/TiO$_2$ is lower than that of pure TiO$_2$.
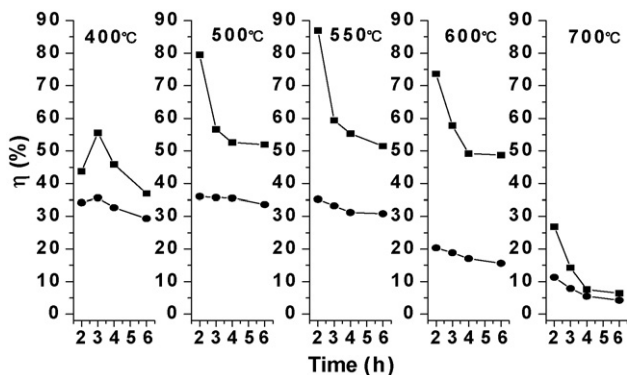

Fig. 4. Effect of heat treatment on the photocatalytic reduction of Cr$_2$O$_7^{2-}$. (■) p-NiO/n-TiO$_2$; and (●) TiO$_2$.
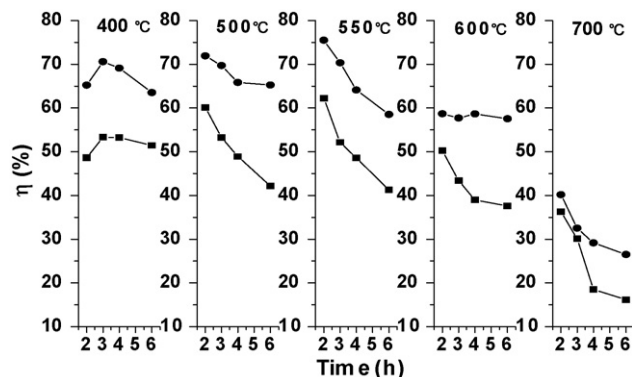
From Fig. 4, it can be seen that, the photocatalytic reduction activities of NiO/TiO$_2$ vary with the change of different heat treatment temperatures and time. In this study, the best preparation condition is about 550 °C for 2 h, and the photoreduction efficiency of Cr$_2$O$_7^{2-}$ can reach 87.0%. The photocatalytic reduction activity of NiO/TiO$_2$ prepared in any other preparation conditions is lower than that of heat treatment at 550 °C for 2 h. From Fig. 5, it is clear that, the change of photocatalytic oxidation activity of NiO/TiO$_2$ is the same as that of the photocatalytic reduction of Cr$_2$O$_7^{2-}$.

It is clear that, the highest photocatalytic activity of NiO/TiO$_2$ exists in an appropriate heat treatment range of 500–600 °C. When the heat treatment temperature is out of this range, the photocatalytic activity of NiO/TiO$_2$ is very low. Furthermore, within this range, there is an optimum heat treatment time at each treatment temperature. For example, when the treatment temperature is 550 °C, the best treatment time is 2 h.

When the heat treatment temperature is 400 °C, the photocatalytic activity of NiO/TiO$_2$ increases with the increase of heat treatment time up to 3 h; when the heat treatment time is higher than 3 h, the photocatalytic activity of NiO/TiO$_2$ decreases gradually with the increase of the heat treatment time; when the heat treatment temperatures are 500 °C and 600 °C, respectively, the photocatalytic activity of NiO/TiO$_2$ decreases with the increase of heat treatment time at the same temperature; when the heat treatment temperature is 700 °C, the photocatalytic activity of NiO/TiO$_2$ decreases rapidly with the increase of heat treatment time.

From Figs. 4 and 5, it can also be seen that, for pure TiO$_2$, the same conclusion is obtained as NiO/TiO$_2$ photocatalyst. But, it is clear that the NiO/TiO$_2$ photocatalyst is highly sensitive to heat treatment temperature and time than that of TiO$_2$, especially for the photocatalytic reduction of Cr$_2$O$_7^{2-}$. For example, when the NiO/TiO$_2$ photocatalyst was heated at temperature 550 °C for 2 h, the photoreduction efficiency is 87.0%; when it was heated at temperature 550 °C for 6 h, the photoreduction efficiency is 51.5%. The photoreduction activity of NiO/TiO$_2$ decreases by 40.8%. For TiO$_2$ photocatalyst, when heated at temperature 550 °C for 2 h, the photoreduction efficiency is 35.2%; when heated for 6 h, the photoreduction efficiency is

30.9%. The photoreduction activity of NiO/TiO_2 decreases by only 12.2%.

The above observations show that heat treatment temperature and time are the important factors that influence the photocatalytic activity of NiO/TiO_2. In this work, when the samples were heated in an appropriate range (500–600 °C) or within in this range, and heated for an optimum time, the photocatalytic activity of NiO/TiO_2 is at its best. It is proposed that in above preparation conditions, the surface of NiO/TiO_2 will not only produce more active sites, but also promote the separation of the photogenerated electrons and holes.

The photocatalytic activity of TiO_2 mainly depends on whether the electron–hole pairs can be separated effectively [28,29]. On the TiO_2 surface, the photoexcited electrons and holes can change in various ways. Among them, the two competitive processes, i.e., capture and recombination, are the most important ones. Photocatalytic reaction is effective only when the photoexcited electrons–holes can be captured. If there are no appropriate capturers of electrons or holes, they will recombine with each other and give off heat inside or on the surface of semiconductor. It is known from the mechanism of separation of electrons and holes that, in order to increase the photocatalytic activity of TiO_2, two important ways should be considered. One is to increase the separation efficiency of the photoexcited electron–hole pairs, and the other is to increase the amount of the photoexcited activity species [30]. For the NiO/TiO_2 photocatalyst, because of the formation of the p–n junction in the NiO/TiO_2, the photogenerated electron–hole pairs are separated by the inner electric field. At the same time, p-type NiO species acts as hole traps and collector [27]. So the p–n junction photocatalyst NiO/TiO_2 has higher photocatalytic reduction activity than that of TiO_2, but lower photocatalytic oxidation activity.

3.3. Characterization of NiO/TiO_2 photocatalyst

Fig. 6 shows the XRD patterns of NiO/TiO_2 and pure TiO_2 heated at different temperatures for 2 h. The amount of doped-NiO is 0.5% (mole ratio of Ni/Ti). From the XRD patterns of NiO/TiO_2, it can be seen that there is only anatase crystal phase present within the appropriate range of heat treatment temperatures (400–600 °C), and there is no diffraction peak of rutile. But when the heat treatment temperature is higher than 600 °C, with an increase of heat treatment temperature, anatase will transfer to rutile gradually. When heat treatment reaches 800 °C for 2 h, the crystal phase of the samples will be transferred into rutile completely.

However, for pure TiO_2, when heat treatment temperature is 400 °C, the XRD pattern shows TiO_2 consists of anatase and rutile. It is clear that, the transformation temperatures from anatase to rutile crystal phase are enhanced greatly when doping NiO into TiO_2. The characteristic diffraction peaks of TiO_2 are connected with heat treatment temperature. As is shown in Fig. 6, it can be seen that, the higher the heat treatment temperature, the stronger the diffraction peaks, and the narrower the peaks become. This indicates that with the increase of the heat treatment temperature, the crystal phase of TiO_2 becomes perfect, and some crystal grains agglutinate and become bigger. The
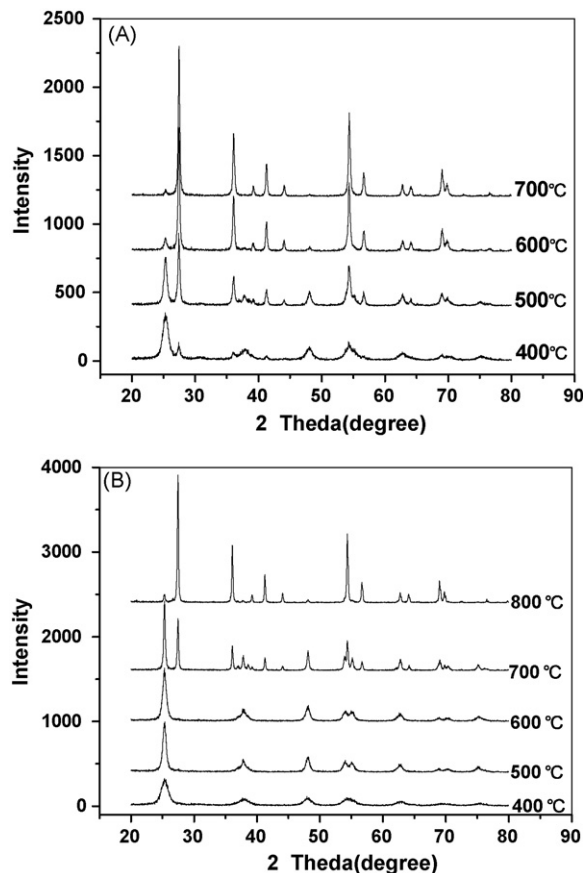

Fig. 6. XRD patterns of pure TiO_2 (A) and p-NiO/n-TiO_2 (B) heated at different temperature.

results also show that when the amount of doped-NiO is 0.5%, the diffraction peaks of NiO cannot be found in XRD patterns. This illustrates that NiO is highly dispersed in the bulk phase of the catalyst. When the amount of doped-NiO is higher than 5.0%, the diffraction peaks of NiO can be found in XRD patterns. It can be calculated by the Scherrer formula that when the samples were heated at 500 °C for 2 h, there is no NiO present, and the average diameter of TiO_2 is about 19.92 nm. When the amount of doped-NiO is 0.5%, the average diameter of NiO/TiO_2 is about 14.33 nm. From the result, it is clear that when doping NiO into TiO_2, the growth of TiO_2 crystal grain is inhibited. This causes the crystalline size decrease and the specific surface area increase. Accordingly, the photocatalytic activity of NiO/TiO_2 photocatalyst is enhanced.

Fig. 7 shows UV–vis diffuse reflection spectra of NiO/TiO_2 and TiO_2, respectively. From Fig. 7, it can be seen that absorption wavelength range of the NiO/TiO_2 is extended greatly towards visible light, compared with pure TiO_2 photocatalyst, and its absorption intensity is also increased a little. The photoexcited wavelength range increases with the increase in the amount of doped-NiO. In theory, because the absorption wavelength range is extended greatly towards visible light and absorption intensity increases, the formation rate of electron–hole pairs on the photocatalyst surface also increases greatly, resulting in the photocatalyst NiO/TiO_2 exhibiting higher photocatalytic activity. From the above results, it is known that the photocatalytic
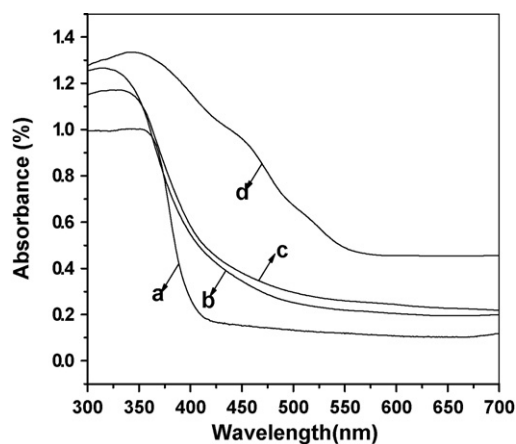
Fig. 7. UV–vis diffuse reflection spectra. (a) TiO$_2$; (b) NiO (0.1%)/TiO$_2$; (c) NiO (0.5%)/TiO$_2$; and (d) NiO (20.0%)/TiO$_2$.

activity of NiO/TiO$_2$ photocatalyst is strongly dependent on the amount of doped-NiO. The photocatalytic reduction activity increases with the increase in the amount of doped-NiO up to 0.5% (mole ratio of Ni/Ti). There is no evident relationship between the photocatalytic activity of NiO/TiO$_2$ photocatalyst and photoexcited wavelength range. Namely, widening photoexcited wavelength range does not increase photocatalytic activity of the photocatalyst in the experimental condition.

Fig. 8 shows higher resolution scanning XPS spectra of Ni 2p and O 1s, respectively. It can be seen that, from XPS spectra of the NiO/TiO$_2$ (omit), the photoelectron peak for Ti 2p
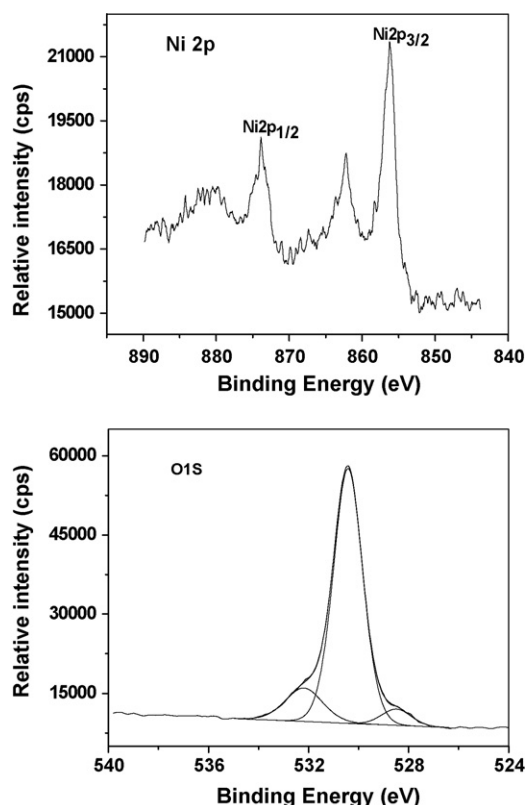

Fig. 8. Higher resolution scanning XPS spectra of Ni 2p and O 1s.

appears clearly at the binding energy of 459.0 eV. The photoelectron peaks of O 1s and Ni 2p are at the binding energies of 529 and 856.2 eV, respectively. It is known that the photoelectron peaks of Ni^{3+} and Ni are at the binding energy of 857.3 and 852.6–852.8 eV, respectively. It is proposed that the binding energy of 856.2 eV is assigned to Ni^{2+}. In order to further determine the oxidation state of the doped nickel, ion chemical analysis was used. The result shows that the doped nickel exists in the form of Ni^{2+}.

From the high resolution scanning XPS spectra of Ni 2p, it is clear that the spectra can roughly be divided into two edges split, referred to as 2p$_{1/2}$ ($\approx$870–885 eV) and 2p$_{3/2}$ ($\approx$845–869 eV) edges, respectively. Ni 2p XPS is assigned to Ni^{2+}. Similar results were reported in Refs. [31,32]. There is no obvious difference between the peaks of the sample before and after photocatalytic reaction, which indicates that the oxidation state of nickel remains stable in the reaction process. From high resolution scanning XPS spectra of O 1s in Fig. 8, it can be seen that oxygen on the sample surface exists at least in three forms with the following binding energies 530.4, 528.5 and 532.2 eV. While the main peak at 530.4 eV is attributed to O lattice of TiO$_2$ since it is seen at the same position as that of the O 1s peak of many rutile and anatase TiO$_2$ surfaces [6,33], that at 528.5 eV is not clear. Freshly cleaved NiO crystal shows an O 1s peak 529.5 or 1 eV below that of TiO$_2$ [34]. It is thus plausible that this O 1s peak is related to NiO particles or of oxygen atoms at the vicinity of both Ni and Ti atoms. The peak at 532.2 eV is most likely due to irreversibly adsorbed water molecules on the surface. It is just because so much adsorption oxygen exists on the TiO$_2$ surface that they become captives of photogenerated electron–hole pairs directly or indirectly. Therefore, recombination of the photogenerated electron–hole pairs is suppressed, and the quantum efficiency of photocatalytic reaction is improved.

4. Conclusions

The p–n junction NiO/TiO$_2$ photocatalysts were prepared by the sol–gel method using Ni(NO$_3$)$_2$·6H$_2$O and tetrabutyl titanate as the raw materials. The photocatalytic reduction activity of NiO/TiO$_2$ photocatalysts is higher than that of the pure TiO$_2$. However, the photooxidation activity of NiO/TiO$_2$ photocatalyst is much lower than that of TiO$_2$. Namely, the p–n junction photocatalyst NiO/TiO$_2$ has higher photocatalytic reduction activity, but lower photocatalytic oxidation activity. The optimum amount of doped-NiO is 0.5% (mole ratio of Ni/Ti). The addition of NiO not only increases transformation temperature from anatase to rutile, but also prevents the growth of TiO$_2$ granule. As the formation of p–n junction NiO/TiO$_2$ photocatalyst and p-type NiO species acts as hole traps and collector, the photogenerated electron–hole pairs are separated by the inner electric field, and the photocatalytic reduction activity is enhanced greatly.

Acknowledgements

References

[1] M.R. Hoffmann, S.T. Martin, W.Y. Choi, D.W. Bahnemann, Environmental applications of semiconductor photocatalysis, Chem. Rev. 95 (1995) 69–96.

[2] J. Yu, J.C. Yu, M.K.P. Leung, W. Ho, Effects of acidic and basic hydrolysis catalysts on the photocatalytic activity and microstructures of bimodal mesoporous titania, J. Catal. 217 (2003) 69–78.

[3] X. Wang, W. Lian, X. Fu, J.M. Basset, F. Lefebvre, Structure, preparation and photocatalytic activity of titanium oxides on MCM-41 surface, J. Catal. 238 (2006) 13–20.

[4] C. Zhang, Y.F. Zhu, Synthesis of square Bi_2WO_6 nanoplates as high-activity visible-light-driven photocatalysts, Chem. Mater. 17 (2005) 3537–3545.

[5] L. Cesar, A. Kay, J.A.G. Martinez, M.J. Gratzel, Translucent thin film Fe_2O_3 photoanodes for efficient water splitting by sunlight: nanostructure-directing effect of Si-doping, J. Am. Chem. Soc. 128 (2006) 4582–4583.

[6] S.F. Chen, G.Y. Cao, The preparation of Nitrogen-doped photocatalyst $TiO_{2-x}N_x$ by ball milling, Chem. Phys. Lett. 413 (2005) 404–409.

[7] R. Asahi, T. Morikawa, T. Ohwaki, K. Aoki, Y. Taga, Visible-light photocatalysis in nitrogen-doped titanium oxides, Science 293 (2001) 269–271.

[8] C. Hu, Y. Lan, J. Qu, X. Hu, A. Wang, $Ag/AgBr/TiO_2$ visible light photocatalyst for destruction of azodyes and bacteria, J. Phys. Chem. B 110 (2006) 4066–4072.

[9] M. Anpo, M. Takeuchi, K. Ikeue, Design and development of titanium oxide photocatalysts operating under visible and UV light irradiation: The applications of metal ion-implantation techniques to semiconducting TiO_2 and Ti/zeolite catalysts, Curr. Opin. Solid State Mater. Sci. 6 (2000) 381–388.

[10] Y.S. Chen, J.C. Crittenden, S. Hackney, L. Sutter, D.W. Hand, Preparation of a novel TiO_2-based p–n junction nanotube photocatalyst, Environ. Sci. Technol. 39 (2005) 1201–1208.

[11] M. Sathish, B. Viswanathan, R.P. Viswanath, C.S. Gopinath, Synthesis, characterization, electronic structure, and photocatalytic activity of nitrogen-doped TiO_2 nanocatalyst, Chem. Mater. 17 (2005) 6349–6353.

[12] X. Chen, C. Burda, Photoelectron spectroscopic investigation of nitrogen-doped titania nanoparticles, J. Phys. Chem. B 108 (2004) 15446–15449.

[13] S.U.M. Khah, M. Al-shahry Jr., W.B. Lngler, Efficient photochemical water splitting by a chemically modified n-TiO_2, Science 297 (2002) 2243–2245.

[14] D. Li, H. Haneda, N.K. Labhsetwar, S. Hishita, N. Ohashi, Visible-light-driven photocatalysis on fluorine-doped TiO_2 powders by the creation of surface oxygen vacancies, Chem. Phys. Lett. 401 (2005) 579–584.

[15] C. Martin, I. Martin, V. Rives, L. Palmisano, M. Schiavello, Structural and surface characterization of the polycrystalline system $CrxOy·TiO_2$ employed for photoreduction of dinitrogen and photodegradation of phenol, J. Catal. 134 (1992) 434–444.

[16] S. Ikeda, N. Sugiyama, B. Pal, G. Marcí, L. Palmisano, H. Noguchi, K. Uosaki, B. Ohtani, Photocatalytic activity of transition-metal-loaded titanium (IV) oxide powders suspended in aqueous solutions: Correlation with electron–hole recombination kinetics, Phys. Chem. Chem. Phys. 3 (2001) 267–273.

[17] L. Palmisano, V. Augugliaro, A. Sclafani, M. Schiavello, Activity of chromium-ion-doped titania for the dinitrogen photoreduction to ammonia and for the phenol photodegradation, J. Phys. Chem. 92 (1988) 6710–6713.

[18] L. Palmisano, M. Schiavello, A. Sclafani, C. Martin, I. Martin, V. Rives, Surface-properties of iron-titania photocatalysts employed for 4-nitrophenol photodegradation in aqueous TiO_2 dispersion, Catal. Lett. 24 (1994) 303–315.

[19] T. Sreethawong, Y. Suzuki, S. Yoshikawa, Photocatalytic evolution of hydrogen over mesoporous TiO_2 supported NiO photocatalyst prepared by single-step sol–gel process with surfactant template, Int. J. Hydrogen Energ. 30 (2005) 1053–1062.

[20] H.Y. Lin, Y.F. Chen, Y.W. Chen, Water splitting reaction on NiO/InVO4 under visible light irradiation, Int. J. Hydrogen Energ. 32 (2007) 86–92.

[21] H. Sato, T. Minami, S. Takata, T. Yamada, Transparent conducting p-type NiO thin films prepared by magnetron sputtering, Thin Solid Films 236 (1993) 27–31.

[22] A. Hameeda, M.A. Gondal, Production of hydrogen-rich syngas using p-type NiO catalyst: a laser-based photocatalytic approach, J. Mol. Catal. A: Chem. 233 (2005) 35–41.

[23] I.H. Tseng, W.C. Chang, J.C.S. Wu, Photoreduction of CO_2 using sol–gel derived titania and titania-supported copper catalysts, Appl. Catal. B: Environ. 37 (2002) 37–48.

[24] Y. Yang, X.J. Li, J.T. Chen, L.Y. Wang, Effect of doping mode on the photocatalytic activities of Mo/TiO_2, J. Photochem. Photobiol. A: Chem. 163 (2004) 517–522.

[25] J.C. Yu, J. Yu, J. Zhao, Enhanced photocatalytic activity of mesoporous and ordinary TiO_2 thin films by sulfuric acid treatment, Appl. Catal. B: Environ. 36 (2002) 31–43.

[26] D. Dvoranova, V. Brezova, M. Mazur, M.A. Malati, Investigations of metal-doped titanium dioxide photocatalysts, Appl. Catal. B: Environ. 37 (2002) 91–105.

[27] J. Bandara, H. Weerasinghe, Solid-state dye-sensitized solar cell with p-type NiO as a hole collector, Sol. Energ. Mat. Sol. C 85 (2005) 385–390.

[28] M.I. Litter, Heterogeneous photocatalysis-Transition metal ions in photocatalytic systems, Appl. Catal. B: Environ. 23 (1999) 89–114.

[29] J.G. Yu, Y. Su, B. Cheng, M. Zhou, Effects of pH on the microstructures and photocatalytic activity of mesoporous nanocrystalline titania powders prepared via hydrothermal method, J. Mol. Catal. A: Chem. 258 (2006) 104–112.

[30] S.F. Chen, G.Y. Cao, The effect of different preparation conditions on the photocatalytic activity of TiO_2SiO_2/beads, Sur. Coat. Technol. 200 (2006) 3637–3643.

[31] St. Uhlenbrock, Chr. Scharfschwerdt, M. Neumann, G. Illing, H.-J. Freund, The influence of defects on the Ni 2p and O 1s XPS of NiO, J. Phys. Condens. Mater. 4 (1992) 7973–7978.

[32] V. Biju, Ni 2p X-ray photoelectron spectroscopy study of nanostructured nickel oxide, Mater. Res. Bull. 42 (2007) 791–796.

[33] S.D. Senanayake, H. Idriss, Photocatalysis and the origin of life: synthesis of nucleoside bases from formamide on TiO_2 (0 0 1) single surfaces, PNAS 103 (2006) 1194–1198.

[34] M. Oku, H. Tokuda, K. Hirokawa, Final states after Ni 2p photoemission in the nickel-oxygen system, J. Electron Spectrosc. Relat. Phenom. 53 (1991) 201–202.